Heliyon 7 (2021) e06932

Contents lists available at ScienceDirect

Heliyon

journal homepage: www.cell.com/heliyon

Research article

Protective effect of nano vitamin D against fatty degeneration in submandibular and sublingual salivary glands: A histological and ultrastructural study

Rasha Hamed Al-Serwi [a,b,**], Mohamed El-Sherbiny [d,e], Mohamed Ahmed Eladl [f,*], Ashwag Aloyouny [a], Ishrat Rahman [a]

[a] Basic Dental Sciences, College of Dentistry, Princess Nourah Bint Abdulrahman University, Riyadh 84428, Saudi Arabia
[b] Oral Biology Department, Faculty of Dentistry, Mansoura University, Mansoura 35516, Egypt
[d] Department of Basic Medical Sciences, College of Medicine, AlMaarefa University, Riyadh 71666, Saudi Arabia
[e] Anatomy Department, Faculty of Medicine, Mansoura University, Mansoura, Egypt
[f] Department of Basic Medical Sciences, College of Medicine, University of Sharjah, Sharjah, United Arab Emirates

ARTICLE INFO

Keywords:
Salivary gland
Submandibular
Sublingual
Rat
Histology
Nano vitamin D
High-fat diet
Degeneration

ABSTRACT

Background: Poor nutritional habits and a low level of physical activity are associated with obesity, leading to increased caloric and fat intakes. A high-fat diet can significantly impact oral health through the accumulation of lipids in the salivary glands, which ultimately affect salivary gland function. Recently, an increasing number of supplement nano-formulations, such as nano vitamin D, have become available. However, only few studies have explored the effects of nano vitamin D on the maintenance of oral health.

Objective: This study aimed to compare the histological effects of nano vitamin D to those of regular vitamin D on fatty degeneration in submandibular and sublingual salivary glands using a rat model.

Methods: Twenty-four adult male albino Sprague–Dawley rats were divided into the following groups: untreated group, high-fat diet group, high-fat diet and regular vitamin D group, and high-fat diet and nano vitamin group. Thereafter, samples of the submandibular and sublingual salivary glands were dissected for histological and electron microscopic studies. Morphometric digital image analysis was used to quantitatively measure the changes in the size and number of acini and secretory granules.

Results: Regular vitamin D had a partial protective effect. However, vitamin D could fully restore cellular structures to their normal state, thereby protecting against fatty degeneration of the salivary tissue and immune cell infiltration, particularly in the submandibular serous tissue. Nano vitamin D was more efficacious than regular vitamin D at restoring the number and size of submandibular serous secretory granules.

Conclusion: Employing nano vitamin D as a supplement to high-fat diets could protect against high-fat diet-induced salivary gland damage in rats.

1. Introduction

Lipids and carbohydrates are essential molecules for energy supply. However, poor nutritional habits and a low level of physical activity lead to obesity and its comorbidity, insulin resistance [1]. Many studies have found that lipids are key in the onset of peripheral tissue dysfunction (e.g., skeletal muscle, heart, and liver) and insulin resistance [2, 3, 4]. Interestingly, the salivary glands of diabetic rats are known to accumulate cytoplasmic lipid droplets of various sizes [5]. Fat accumulation is a crucial trigger of an inflammatory immune response, indirectly causing oral swelling, inflammation, and extreme pain, even when talking and chewing [6].

The major salivary glands in humans comprise the parotid, sublingual, and submandibular glands. The parotid gland is serous in both humans and rodents. The human submandibular gland is a mixed gland composed of both serous and mucous acinar cells, whereas the rodent submandibular gland only has the serous type. Finally, the sublingual glands of both humans and rodents comprise mixed types of glands,

* Corresponding author.
** Corresponding author.
E-mail addresses: r_al_serwi@hotmail.com (R.H. Al-Serwi), meladl@sharjah.ac.ae (M.A. Eladl).

https://doi.org/10.1016/j.heliyon.2021.e06932
Received 14 September 2020; Received in revised form 17 November 2020; Accepted 23 April 2021

including two major types of secretory cells: serous and mucous cells. The mucous acini primarily produce mucins, mainly O-linked glycoproteins, which function to lubricate and protect by forming a barrier in the oral cavity and around its structures. Serous acini produce N-linked glycoproteins and specific functional proteins, such as alpha-amylase, antimicrobials, and calcium-binding proteins [7, 8].

As reported, characteristic histological changes in the salivary gland parenchyma can occur due to local or systemic conditions [9]. Fatty tissue is an intrinsic parenchymal component of the salivary glands [10]. Changes in fat content are associated with several diseases, including malnutrition [11], alcoholism [12], Sjögren's syndrome [13], pseudo-Sjögren's syndrome [9], lipomatosis [14], and radiation injury after radiation therapy [15]. A high-fat diet can significantly affect oral health by causing lipid accumulation in the salivary glands, leading to dysfunctional salivary glands or even triggering autoimmune disorders, such as Sjögren's syndrome [13].

Vitamin D is a fat-soluble vitamin that is mainly obtained via exposure of the skin to sunlight, resulting in cholecalciferol (vitamin D3) from dehydrocholesterol or dietary sources in the form of ergocalciferol (vitamin D2), which originate from plants or vitamin D3 from animal material. Both vitamins D2 and D3 are subsequently hydroxylated in the liver and kidneys to calcitriol (1,25-ihydroxycholecalciferol), the active form of vitamin D [16]. Various preparations of vitamin D are available in the market. Two of the most competitive types are regular vitamin D and nano vitamin D. The critical difference between these two preparations is the lipid particle size in the formulations. Nano vitamin D is more readily absorbed in the intestines than the standard emulsion vitamin D [17]. It is also taken up into circulation more efficiently. As a result, nano vitamin D is more readily distributed to tissues with higher bioavailability [18].

Nano vitamin D increases blood vitamin levels almost three-fold higher than regular vitamin D [19]. The active form of vitamin D has hormone-like functions. In addition to its dominant role in regulating plasma Ca^{2+} and phosphorus levels, it also plays a role in many other physiological processes, including the modulation of the immune system and the control of cell proliferation and differentiation [16]. Vitamin D deficiency is associated with inflammation and has been attributed to an increasing number of chronic disease conditions related to autoimmune diseases, cardiovascular diseases, and fatty liver, among others [20, 21, 22, 23]. Vitamin D deficiency has also been linked to obesity and the onset of obesity-associated diseases [24, 25]. Furthermore, vitamin D treatment is associated with decreased insulin resistance [26].

Very few studies have explored the histological effects of intracellular lipid droplet accumulation in the salivary glands. Of note, changes in the structure and function of the salivary gland can increase the number of oral conditions. As vitamin D can help to maintain organ function and protect against disease and dysfunction, the present study aimed to assess, in detail, the histological effects of nano vitamin D versus regular vitamin D in fatty degeneration of the salivary gland using an animal (Sprague–Dawley rats) high-fat model [24, 25].

2. Material and methods

2.1. Drugs

Nanoemulsion vitamin D3 was prepared by the University of Illinois at Urban-Champaign, as reported previously [23, 27]. Briefly, a pea protein isolate (PPI) was prepared from dry yellow peas using a wet extraction process. The soluble pea protein extract was tested for its water solubility, turbidity, surface hydrophobicity, free sulfhydryl (SH) group content, and particle size. Samples were also analyzed using sodium dodecyl sulfate-polyacrylamide gel electrophoresis (SDS-PAGE) to determine the molecular weight of the proteins. Tandem pH shifting to pH 12 and ultrasound treatment (U5) were found to yield the highest solubility. These samples were subsequently used to prepare nano-emulsions using a stock of 1.04% cholecalciferol in canola oil loaded into PPI with a maximum loading capacity of 1.5 ± 0.2 μg/mg pea protein [27]. Vidrop was employed as an aqueous oral form of regular vitamin D3 (Medical Union Pharmaceuticals AbuSultan, Ismailia, Egypt).

2.2. Animals

The ethics committee at the Mansoura Experimental Research Centre (MERC), Mansoura University in Egypt, approved the experimental work (I.R.B. no. 316-2017) and provided ethical guidelines for the study. The sample size was based on a previously published study with a similar experimental design [23]. Twenty-four adult male albino Sprague–Dawley rats (Theodor Bilharz Research Institute, Imbaba, Egypt; age, 8–10 weeks; weight, 200–250 g) were used according to the National Institutes of Health Guide for the Care and Use of Laboratory Animals. The rats were housed in a metal meshed cage (3 per cage) in a controlled environment with a 12 h light/dark cycle at a regulated temperature between and 22–23 °C and humidity between 65-70%. Animals had free access to drinking water at all times. Six rats were randomly assigned to one of the following groups: untreated group, high-fat diet group, high-fat diet and regular vitamin D group, and high-fat diet and nano vitamin group. The untreated group was maintained on a normal healthy diet with standard chow (Formula Diet 5008, $P^{M.I.T.M.}$; Nutrition International, Richmond, Indiana). The high-fat diet group was maintained on a high-fat diet to induce fatty dysfunctional salivary glands; the high-fat diet consisted of corn oil containing over 98% ω-6 polyunsaturated fatty acids (P.U.F.A.). The diet consisted of 21.4% fat, 17.5% protein, 50% carbohydrate, 3.5% fiber, and 4.1% ash. The high-fat diet and regular vitamin D group received regular vitamin D (40 IU/kg of body weight orally/day) in addition to a high-fat diet. The high-fat diet and nano vitamin group received nano vitamin D (40 IU/Kg of body weight orally/day), in addition to the high-fat diet. Rats in groups of high-fat diet group, high-fat diet and regular vitamin D group, and high-fat diet and nano vitamin group were fed orally via daily gastric intubation (5 g/100 g body weight/day) between 7-9 am with the doses indicated randomly; fed rats were transferred to a new cage to minimize errors. The diets and treatments were concurrently maintained for 12 weeks [23]. The use of gastric intubation ensured that all rats had a similar level of fatty induction and reduced errors in judgment regarding the effects of vitamin D.

2.3. Histopathological sample preparation

The samples were obtained as previously described [23]. Briefly, animals were sacrificed by decapitation at the end of the experimental animal study. Thereafter, the submandibular and sublingual salivary glands were dissected and carefully sectioned into two pieces for subsequent use in the histopathological analysis and transmission electron microscopy (TEM) analysis. Specimens from the salivary glands were fixed in 10% neutral buffered formalin for 12 h at room. After fixation, specimens were dehydrated in an ascending series of alcohol, cleared in two xylene changes, and embedded in molten paraffin. Sections of 5-μm thickness were obtained using a rotary microtome (Leica Biosystems, Buffalo Grove, Illinois, USA) and mounted on clean slides. For histological examination, the salivary sections were stained with hematoxylin and eosin (H&E) (Life Chemicals group, Alexandria, Egypt) [28]. A blinded histopathological specialist performed a descriptive analysis of all H&E slides to determine the histological changes in the serous and mucous salivary tissues.

2.4. Electron microscopic study

The salivary gland specimens were fixed in 2.5% glutaraldehyde solution for 12 h and post-fixed in 1% osmium tetroxide for 2 h. After dehydration and embedding in epoxy resin, the specimens were cut into semi-thin (2 μm) sections and subsequently examined with a transmission electron microscope (J.E.O.L., JEM-2100; Tokyo, Japan, Electron

Microscopic Unit, Mansoura University). Descriptive analysis was performed to determine subcellular changes in the serous and mucous acini by a blinded histopathological specialist [29].

2.5. Morphometric study and digital analysis

The submandibular and sublingual salivary gland sections were analyzed using light microscopy with an Olympus CX22 microscope (Olympus, Tokyo, Japan). Photographs of the slides were captured using a ToupCam digital camera (model no.: XCAM1080PHA; ToupTek, Hangzhou, China) attached to the microscope. Digital images of H&E staining (10 cm wide and 5 cm long from 8 random fields of view (6 per group)) were collected at 400× magnification. The saved TIFF image files were analyzed using the video test morphology software (VideoTesT, St Petersburg, Russia). The perimeters of serous submandibular acini and sublingual mucous acini were randomly chosen to record the acini cell number and acini cell area calibrated from the H&E slides. TEM images of the apical areas of the serous and mucous acini were randomly chosen, and the number of secretory granules and the granular area were analyzed and photographed using the same optical system under the same conditions. Measurements of the area were recorded and exported as an Excel file in μm^2 for H&E digital analysis and TEM digital analysis. For each *n* number, eight fields of view were recorded (6/group).

2.6. Statistical analysis

Statistical data analysis was performed using GraphPad PRISM 8 software (San Diego, California, USA). One-way ANOVA followed by Tukey's post-hoc multiple comparison test was used to compare the means of the groups. All analyses were carried out at a p-value equal to 0.05, with a 95% confidence interval (CI). Statistical significance is indicated by asterisks (*) in tables and numbers in the figures.

3. Results

3.1. Light microscopic findings

3.1.1. Light microscopic analysis of the submandibular salivary gland

The untreated group had the typical histological architecture of serous acini with connective tissue stroma, duct system, and granular convoluted tubules. As expected, the high-fat diet group displayed a decrease in acinar cell numbers, with a loss of the usual round outlines, pyknotic darkly stained nuclei, and multiple vacuolizations within the acinar cells. Moreover, the cellular remnants were scattered throughout the gland. An increased number of hypertrophied, irregular outlines of granular convoluted tubules with signs of degeneration, cytoplasmic vacuolization, and inflammatory cellular infiltration were evident. In the high-fat diet and regular vitamin D group, restoration of acinar architecture was observed, with deeply stained nuclei despite variable degrees of minor cytoplasmic vacuolization, in addition to well-formed granular convoluted tubules. Interestingly, in the high-fat diet and nano vitamin group, acinar cells showed homogenous cytoplasm, few vacuoles, and intact multiple granular convoluted tubules (Figure 1).

Light microscopic analysis of the untreated sublingual salivary gland showed normal mucous acini cells with pale basophilic spongy cytoplasm, flattened basal nuclei, and healthy connective tissue stroma with a duct system. In contrast, the high-fat diet group displayed densely packed mucous acinar cells with irregularly shaped giant acini, thickened and fibrotic connective tissue septa, and cellular infiltration. In contrast, the high-fat diet and regular vitamin D group exhibited packed mucous

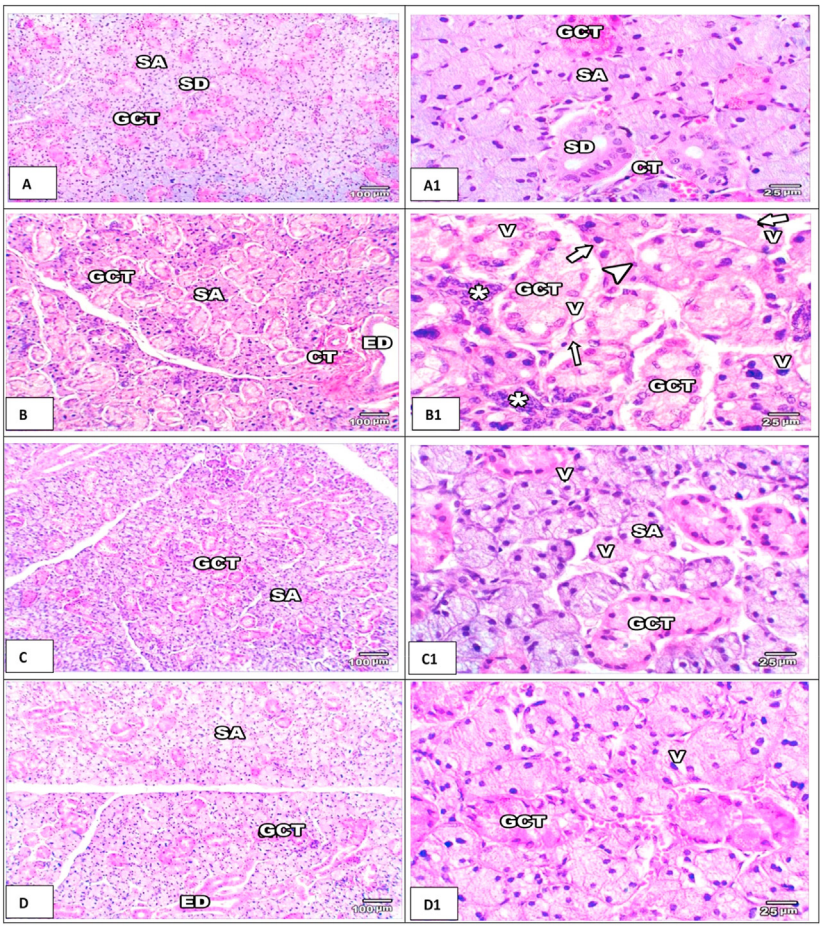

Figure 1. Histological image of the submandibular salivary gland serous acini stained with H&E. The untreated group **(Panel A, A1)** has serous acini (S.A.) with spherical basal nuclei. The connective tissue stroma (C.T.) has striated ducts (S.D.) separated by thin inter-acinar connective tissue. Granular convoluted tubules (G.C.T.) appear with granular cytoplasmic content. The high-fat diet group **(Panel B, B1)** shows a decrease in acinar cells (S.A.) with a loss of the regular round outlines (black arrow), pyknotic darkly stained nuclei (arrowhead), multiple vacuolizations within the acinar cells (V), and cellular remnants scattered throughout the gland (white arrow). An increase in the number of hypertrophied irregular outlines of granular convoluted tubules (G.C.T.) with signs of degeneration and cytoplasmic vacuolization (V) and inflammatory cellular infiltration (asterisks) is observed. The high-fat diet and vitamin D group **(Panel C, C1)** shows restored acinar architecture with deeply stained nuclei (S.A.) despite variable degrees of minor cytoplasmic vacuolization (V). Well-formed granular convoluted tubules (G.C.T.) are observed. The high-fat diet and nano vitamin D group **(Panel D, D1)** shows acinar cells (S.A.) with homogenous cytoplasm, few vacuoles (V), and intact multiple granular convoluted tubules with an increase in its granular content (G.C.T.). Note: The excretory ducts have a healthy cell lining and clear lumen (E.D.).

acinar cells with few giant acini, decreased fibrotic connective tissue septa, and no cellular infiltration. Meanwhile, the high-fat diet group and nano vitamin D showed the mucous acini and duct system; wide spaces between the acini were clear with no fibrotic connective tissue or cellular infiltrates, and fewer giant acini were observed (Figure 2).

3.2. Electron microscopic findings

When the submandibular salivary serous tissue was examined by TEM, the untreated group was found to display regular-shaped serous acinar cells with a vesicular nucleus and secretory granules of different electron densities. We observed ultrastructural changes with marked cell organelle degeneration in the high-fat diet group, leaving only few strands of rough endoplasmic reticulum, small darkly stained degenerated mitochondria lipid droplet deposition, and deformed dense nuclei. The number of secretory granules decreased and appeared to fuse with each other. The high-fat diet and regular vitamin D group showed serous acinar cells clustered with an irregularly shaped electron-dense nucleus, immature light, dense serous granules, few intracytoplasmic vacuolizations, and reduced lipid deposition. Meanwhile, the high-fat diet and nano vitamin D group had preserved and relatively healthy active secreting acinar cells, despite the presence of one to two lipid droplets in few of the acinar cells (Figure 3).

The untreated sublingual salivary mucous tissue had mucous acinar cells with an open-faced nucleus, numerous lightly stained lucent secretory granules, and mitochondria with parallel patterns of crests. In contrast, the high-fat diet group had acinar cells with malformed nuclei and various alterations in the cytoplasmic organelles, including decreased secretory granules, cell organelle degeneration, dilated Golgi apparatus, intracytoplasmic vacuolization, and lipid droplet deposition. Compared to the untreated group, the high-fat diet and regular vitamin D group had an intact nucleus, with decreasing numbers of specific light mucous secretory granules. Few cytoplasmic vacuolizations, lipid droplet depositions, and wide interacinar spaces were also evident in this group. Interestingly, the high-fat diet and nano vitamin D group had a healthy appearance of acinar cells encircling the lumen, with an intact nucleus and cluster of electron-lucent mucous secretory granules. Few cytoplasmic vacuolisations were observed (Figure 4).

3.3. Digital analysis of H&E staining

Descriptive statistics were performed for the digital analysis of H&E staining to derive the mean acinar cell number and mean area of the acinar cells (Table 1, Figure 5). The average number of submandibular serous acini cells was significantly lower ($p < 0.001$) in the high-fat diet group (10 ± 2.5) than in the untreated group (34 ± 4.2). In contrast, there was a significant increase ($p < 0.001$) in the number of submandibular serous acini cells in both the high-fat diet groups administered regular vitamin D (28 ± 3.1) and those administered nano vitamin D (35 ± 4.3). The group treated with nano vitamin D (35 ± 4.3) also had a significant increase ($p < 0.05$) in the average number of submandibular serous acini cells compared to the group treated with regular vitamin D (28 ± 3.1). With regards to the average area of the submandibular serous acini, there was a significant increase ($p > 0.05$) in the high-fat diet group (3950 ± 816.4) compared to that in the untreated group (2765 ± 493.6). In contrast, a significant decrease ($p < 0.05$) was observed in the high-fat diet and regular vitamin D group (2819 ± 553.6) and the high-fat diet and nano vitamin D group (2941 ± 462.3). However, there was no significant difference ($p > 0.05$) between treatment with regular vitamin D (2819 ± 553.6) and nano vitamin D (2941 ± 462.3). With regards to the average number of sublingual mucous acini cells, there was a significant decrease ($p < 0.05$) in the high-fat diet group (17 ± 4) compared to the untreated group (23 ± 2.5). In contrast, there was a non-significant increase ($p > 0.05$) in both the high-fat diet groups administered regular

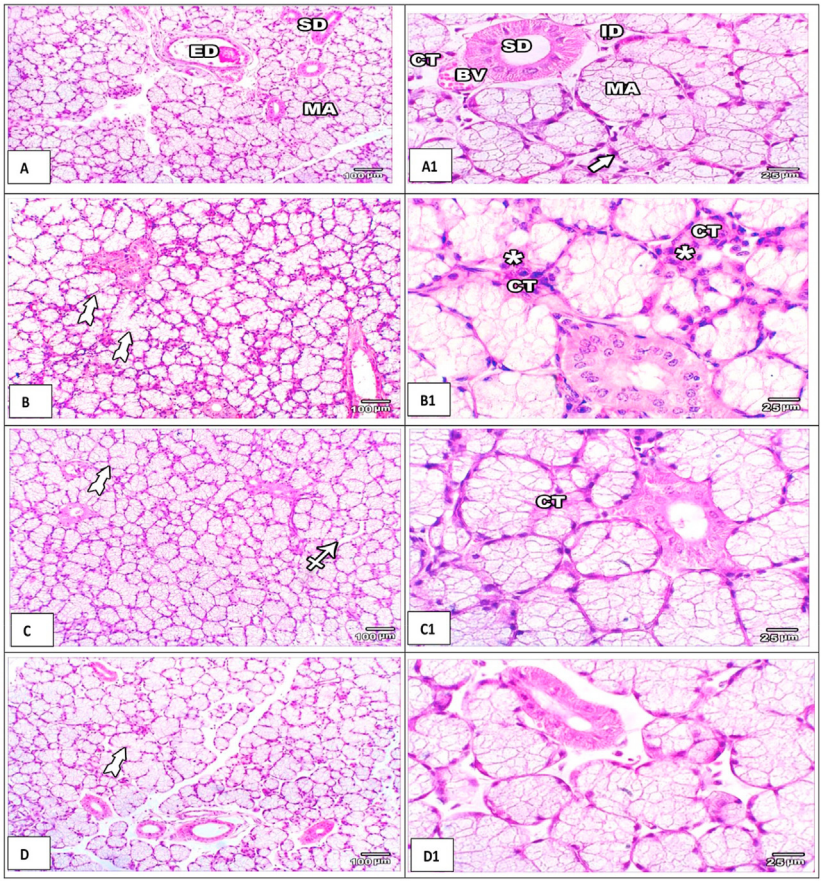

Figure 2. Histological images of the sublingual salivary gland mucous acini stained with H&E. The untreated group **(Panel A, A1)** has mucous acini (M.A.) with pale basophilic spongy cytoplasm, flattened basal nuclei, and myoepithelial cells (black arrow) grasping the acini. The connective tissue stroma (C.T.) has an intercalated duct (I.D.), striated ducts (S.D.), and an execratory duct (E.D.). The high-fat diet group **(Panel B, B1)** has densely packed mucous acinar cells with irregularly shaped giant acini (white arrows). Thickened and fibrotic connective tissue septa (C.T.) with cellular infiltration (asterisks) and diminished and/or absent interlobular spaces are observed. The high-fat diet and vitamin D group **(Panel C, C1)** has packed mucous acinar cells with some giant acini (white arrow); a decrease in the fibrotic connective tissue septa (C.T.) with no cellular infiltration and the interlobular spaces has started appearing (dotted arrow). The high-fat diet and nano vitamin D group **(Panel D, D1)** shows the typical general architecture of the mucous acini and duct system. The wide area between the acini is clear, with no fibrotic connective tissue or inflammatory cells observed. Note: Few giant acini are observed (white arrow).

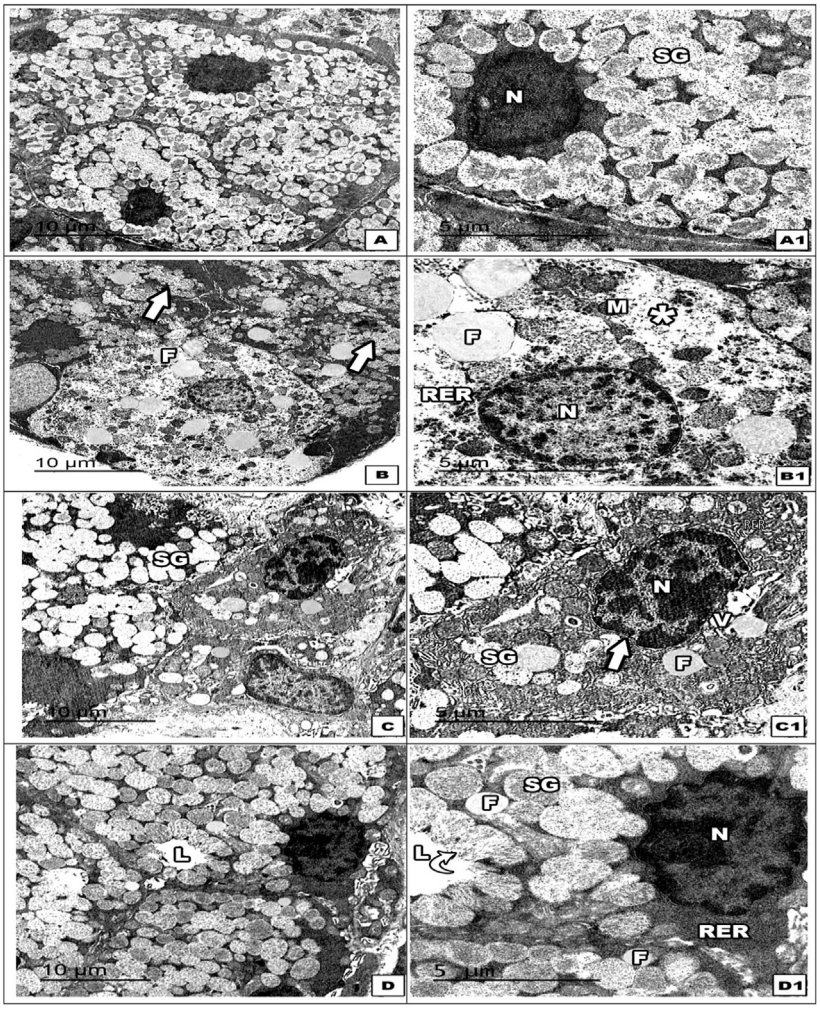

Figure 3. Electron micrograph image of the submandibular salivary gland serous acini. The untreated group **(Panel A, A1)** shows regular-shaped serous acinar cells with a vesicular nucleus (N) and secretory granules with different electron densities (S.G.). The high-fat diet group **(Panel B, B1)** has acinar cells with marked cell organelle degeneration (asterisk), leaving few strands of rough endoplasmic reticulum (R.E.R.), small darkly stained degenerated mitochondria (M), lipid droplet deposition (F), and deformed dense nuclei (N). Note: The number of secretory granules decreased, and the granules appeared to fuse with each other (white arrows). The high-fat diet and vitamin D group **(Panel C, C1)** has serous acinar cells clustered with irregular-shaped electron-dense nucleus (N), immature light, dense serous granules (S.G.), few intracytoplasmic vacuolizations (V), and decreased lipid deposition (F). The high-fat diet and nano vitamin D group **(Panel D, D1)** shows active secreting acinar cells with a vesicular nucleus (N) surrounded by parallel arrays of the rough endoplasmic reticulum (R.E.R.). Numerous round, mature, and immature serous secretory granules (S.G.) in the process of releasing their content into the lumen (curved arrow) are observed. Note: The absence of cytoplasmic vacuolization and one to two lipid droplets are observed (F).

vitamin D (23 ± 4.5) and those administered nano vitamin D (22 ± 1.7). With regards to the average area of the sublingual mucous acini, there was a non-significant difference ($p > 0.05$) between the untreated (4232 ± 408.3), high-fat diet (4920 ± 867.6), and treated groups administered regular vitamin D (4465 ± 724.8) and those administered nano vitamin D (4616 ± 800.7).

3.4. Digital analysis of the TEM images

Descriptive statistics were performed for the digital analysis of TEM images to derive the mean secretory granule number and the mean area of granules relative to untreated granules (Table 2 and Figure 6). With regards to the average number of secretory granules of submandibular serous acini cells, there was a markedly significant decrease ($p < 0.001$) in the high-fat diet group (7 ± 2.3) compared to the untreated group (95 ± 4.6). In addition, there was a significant increase ($p < 0.001$) in both the high-fat diet-treated groups with regular vitamin D (37 ± 5.2) and nano vitamin D (66 ± 5.5). Meanwhile, there was a markedly significant increase ($p < 0.001$) in the group treated with nano vitamin D (66 ± 5.5) and the group treated with regular vitamin D (37 ± 5.2). Regarding the average area of the submandibular serous acini, there was a markedly significant decrease ($p < 0.001$) in the high-fat diet group (217 ± 69.9) compared to the untreated group (726 ± 90.96) and a markedly significant increase ($p < 0.01$) in the high-fat diet and regular vitamin D group (423 ± 105.4) and the high-fat diet and nano vitamin D group (705 ± 113.4). Meanwhile, a significant increase ($p < 0.005$) in the group treated with nano vitamin D (705 ± 113.4) was observed relative to the group treated with regular vitamin D (423 ± 105.4). Regarding the average number of secretory granules of sublingual mucous acini cells, there was a markedly significant increase ($p < 0.001$) in the high-fat diet group (71 ± 4.8) relative to the untreated group (33 ± 4.8), and in the high-fat diet groups administered regular vitamin D (63 ± 3.6) and nano vitamin D (88 ± 4.6) compared to the untreated group (33 ± 4.8). However, there was a significant decrease ($p < 0.05$) in the number of these cells in the high-fat diet group treated with regular vitamin D (63 ± 3.6) and a significant increase ($p < 0.001$) in the high-fat diet group treated with nano vitamin D (88 ± 4.6) compared to the high-fat diet group (71 ± 4.8). For the average area of the secretory granules of sublingual mucous acini, there was a markedly significant decrease ($p < 0.001$) in the high-fat diet groups (743 ± 123.6) treated with regular vitamin D (930 ± 111.5) and nano vitamin D (1350 ± 138.7) compared to the untreated group (3861 ± 394.6). However, there was a non-significant increase ($p > 0.05$) in the high-fat diet group treated with regular vitamin D (930 ± 111.5) and Nano vitamin D (1350 ± 138.7) compared to untreated group (3861 ± 394.6). Meanwhile, there was a significant increase ($p < 0.005$) in the high-fat diet group treated with nano vitamin D (1350 ± 138.7) compared to the untreated high-fat diet group (743 ± 123.6).

4. Discussion

Lipid accumulation impairs tissue organ function in the skeletal muscles and liver, leading to conditions such as obesity and diabetes, among others [2, 3, 4]. Although salivary gland dysfunction is a critical factor in many oral pathological conditions, very few studies have

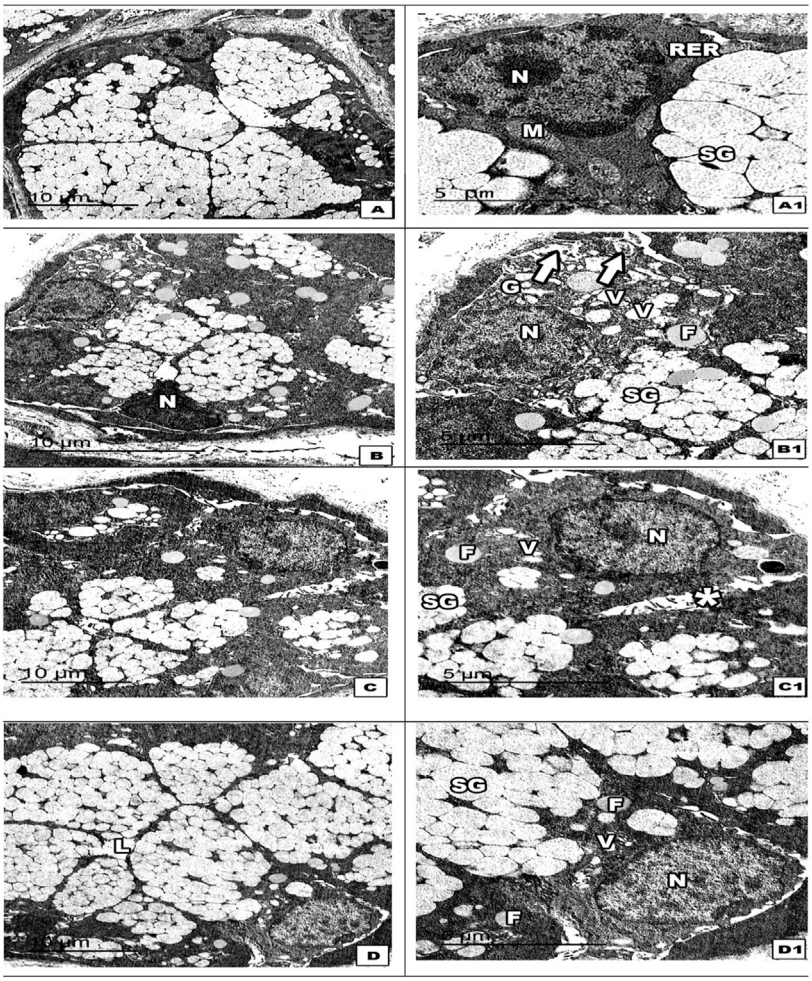

Figure 4. Electron micrograph image of the sublingual salivary gland mucous acini. The untreated group **(Panel A, A1)** has mucous acinar cells with an open-faced nucleus (N) surrounded by parallel arrays of the rough endoplasmic reticulum (R.E.R.), numerous lightly stained, lucent secretory granules, and mitochondria (M) with parallel patterns of crests. The high-fat diet group **(Panel B, B1)** shows acinar cells with malformed nuclei (N) and various alterations in the cytoplasmic organelles, including decreased secretory granules (S.G.), cell organelle degeneration (white arrows), dilated Golgi apparatus (G), intracytoplasmic vacuolization (V), and lipid droplet deposition (F). The high-fat diet and vitamin D group **(Panel C, C1)** shows an intact nucleus (N) and standard light mucous secretory granules, but a decreased number compared to the untreated group. Some cytoplasmic vacuolization (V) and lipid droplet deposition (F) in between is observed. Note: Wide intercellular canaliculi (asterisks). The high-fat diet and nano vitamin D group **(Panel D, D1)** has healthy appearance of acinar cells encircling the lumen (L) with intact nucleus (N) and clusters of electron-lucent mucous secretory granules (S.G.). Note: Few cytoplasmic vacuolizations (V) and one to two lipid droplets are observed (F).

Table 1. Average number and area of submandibular serous and sublingual mucous acini under different treatment conditions.

Groups n	Mean no. of cells	SD	F-value	Mean area of the cell (μm^2)	SD	F-value
Untreated	34	4.2	63.2	2765	493.6	5.2
High-fat diet	10	2.5		3950	816.4	
High-fat diet + vitamin D	28	3.1		2819	553.6	
High-fat diet + Nano vitamin D	35	4.3		2941	462.3	
Untreated	23	2.5	4.2	4232	408.3	1.0
High-fat diet	17	4.0		4920	867.6	
High-fat diet + vitamin D	23	4.5		4465	724.8	
High-fat diet + Nano vitamin D	22	1.7		4616	800.7	

reported the lipid composition of the sublingual and submandibular salivary glands and the possible effects of excess lipid deposition on its function. Indeed, lipid accumulation may play a significant role in fatty degeneration of the salivary glands.

Currently, the application of nanotechnology is revolutionizing science and medicine. Nanomaterials can enhance the effectiveness of diagnostic and therapeutic procedures and support the advancement of drug discovery and delivery [30, 31]. In the present study, high-fat diet-induced cellular and subcellular structural damage to normal acini of the submandibular and sublingual glands was demonstrated in rats. In addition, treatment with both regular vitamin D and nano vitamin D was found to attenuate structural damage caused by a high-fat diet. These results coincide with those of previous studies, indicating the efficacy and bioviability of vitamin D in the salivary gland [32, 33, 34].

Sprague-Dawley rats were used as a model to assess the effects of a high-fat diet, regular vitamin D, and nano vitamin D to shed light on the activities and effects of regular vitamin D and nano vitamin D in humans. The rodent salivary gland may be a suitable model to study the effects of lipid-induced salivary gland dysfunction. Further, any therapeutic interventions evaluated in rats could eventually be translated for use in humans [35].

4.1. Light electron microscope

Our results show that a high-fat diet causes more disruption in the serous acini than the mucous acini, leading to inflammatory cell infiltration, hypertrophy, degeneration of the granular convoluted tubule submandibular gland (H&E staining), and degenerated cell organelles

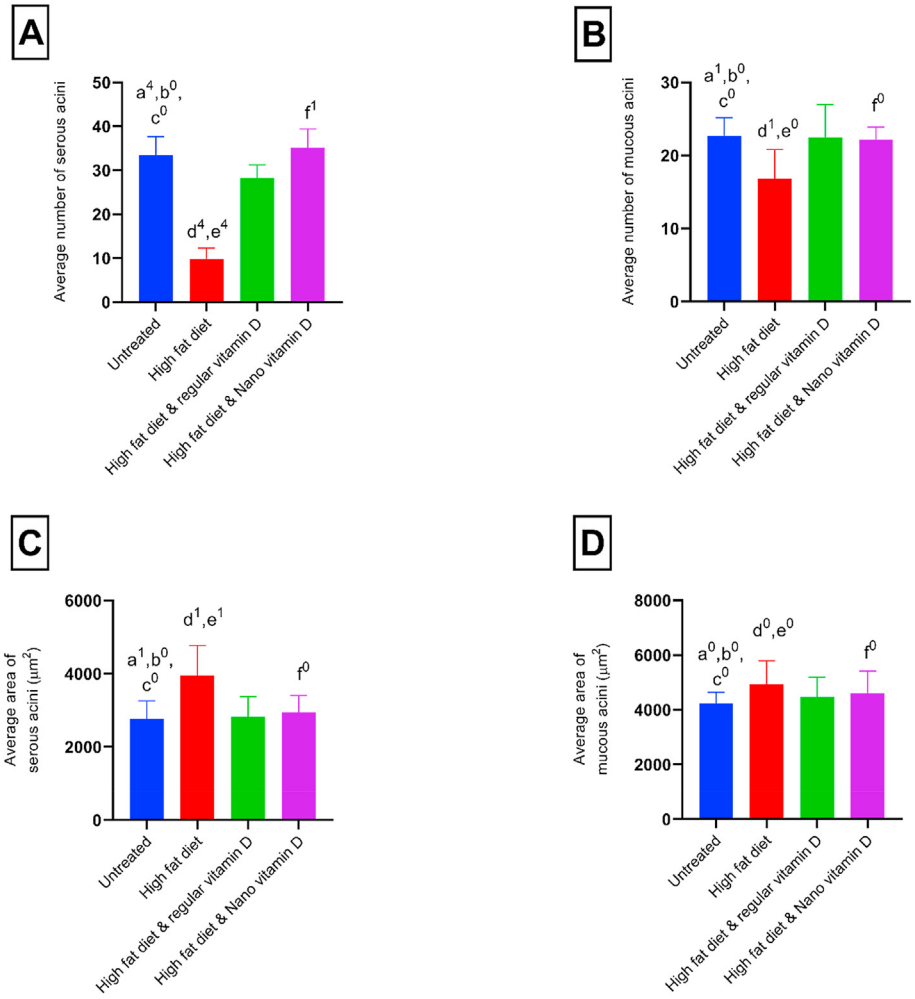

Figure 5. Graph of the average number and area of acini in the submandibular and sublingual salivary glands. Digital morphometric analysis was performed on serous and mucous acini H&E images. (A) Average number of submandibular serous acini. (B) Average number of sublingual mucous acini. (C) Average size of the submandibular serous acini (μm^2). (D) Average size of the sublingual mucous acini (μm^2). Data are presented as mean ± SD. Differences between groups were identified using one-way ANOVA, followed by Tukey's multiple comparison post-test, indicated above the bars. a: comparison between the untreated and high-fat diet group; b: comparison between the untreated and vitamin D group; c: comparison between the untreated and nano vitamin D group; d: comparison between the high-fat diet and vitamin D group; e: comparison between the high-fat diet and nano vitamin D groups; and f: comparison between the vitamin D and nano vitamin D group. Subscript numerals indicate the p-value: $^4p<0.001$, $^3p<0.005$, $^2p<0.01$, $^1p<0.05$, ^{0}no significant difference.

Table 2. Average number and size of secretory granules in submandibular serous and sublingual mucous acini under different treatment conditions.

Groups	Mean no. of granules	SD	F-value	Mean area of granules (nm^2)	SD	F-value
Untreated	95	4.6	408	726	90.96	39.0
High-fat diet	7	2.3		217	64.90	
High-fat diet + vitamin D	37	5.2		423	105.4	
High-fat diet + Nano vitamin D	66	5.5		705	113.4	
Untreated	33	4.8	161	3861	394.6	249
High-fat diet	71	4.8		743	123.6	
High-fat diet + vitamin D	63	3.6		930	111.5	
High-fat diet + Nano vitamin D	88	4.6		1350	138.7	

and lipid droplet deposition (transmission electron microscopy). However, based on H&E staining, the mucous acini of the sublingual salivary gland displayed more densely packed acini than the serous acini forming giant acini, with inflammatory cellular infiltrates similar to those seen in the serous acini with thick fibrous tissue septa.

Cellular and subcellular analyses revealed that nano vitamin D treatment was superior to regular vitamin D treatment at protecting against the high-fat diet-induced degeneration of the serous acini. There was no vacuolization and very few fat droplets compared to those observed in the high-fat diet-treated group. In terms of providing protection against a high-fat diet-induced decline in granular number and reduced size within the serous acini, nano vitamin D showed significantly better effects, being more efficacious than regular vitamin D at increasing granule numbers and protecting against granular degeneration.

The ultrastructure observed in the mucous acini was representative of cytoplasmic vacuolization with lipid deposition and showed signs of organelle degeneration; however, this was to a lesser extent than that observed in the serous acini. It is difficult to explain precisely why a high-fat diet had a less damaging effect on the mucous acini. However, this may be attributed to the innate activity of mucous cells storing and processing higher levels of fat than serous cells. A previous study with a diabetic model showed that degeneration occurred more frequently in the serous acini than in the mucous acini, and this was coupled with lipid accumulation [36]. Interestingly, Matczuk et al. reported a reduction in

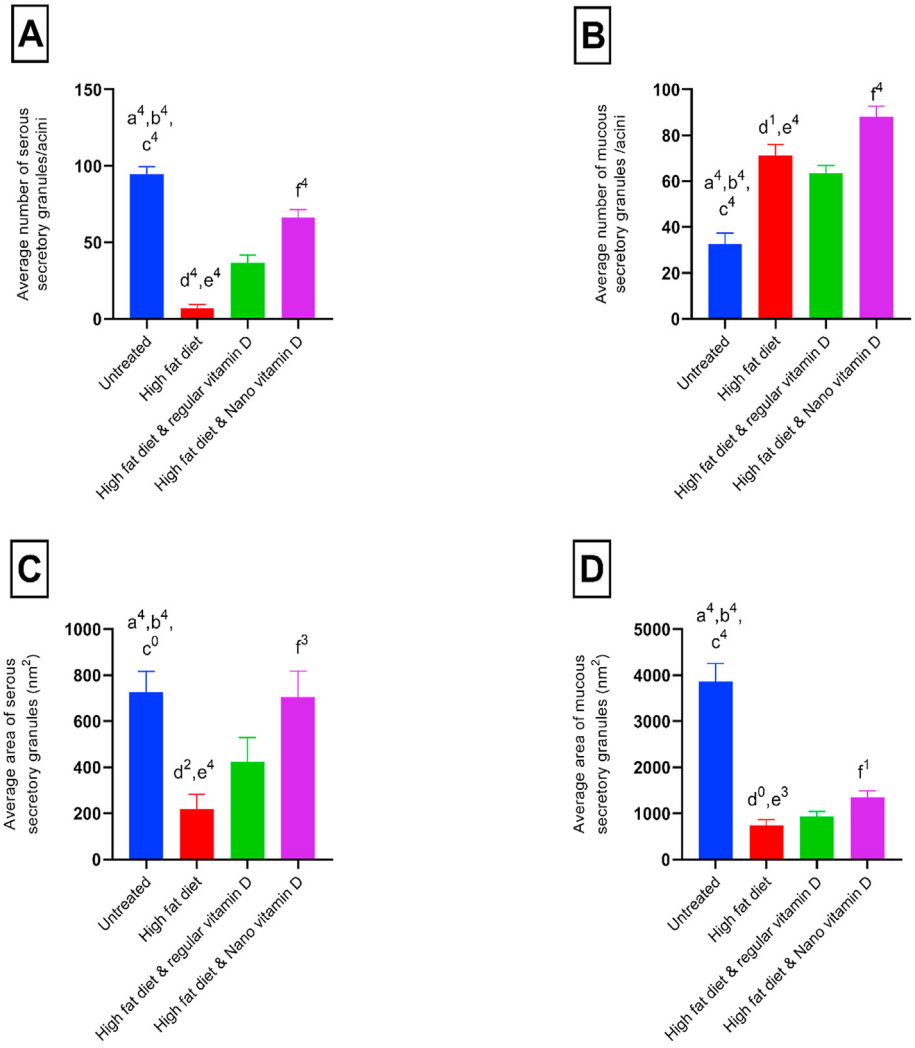

Figure 6. Graph of the average number and area of secretory granules per acini in the submandibular and sublingual salivary glands. Digital morphometric analysis was performed on the serous and mucous TEM images. (A) Average number of submandibular serous secretory granules. (B) Average number of sublingual mucous secretory granules. (C) Average size of the submandibular serous secretory granules (nm^2). (D) Average size of the sublingual mucous secretory granules (nm^2). Data are presented as mean ± SD. Differences between groups were identified using ANOVA, followed by Tukey's multiple comparison post-test, indicated above the bars. a: comparison between the untreated and high-fat diet group; b: comparison between the untreated and vitamin D group; c: comparison between the untreated and nano vitamin D group; d: comparison between the high-fat diet and vitamin D group; e: comparison between the high-fat diet and nano vitamin D group; and f: comparison between the vitamin D and nano vitamin D group. Subscript numerals indicate the p-value: $^4p<0.001$, $^3p<0.005$, $^2p<0.01$, $^1p<0.05$, ^{0}no significant difference.

phospholipid concentration and accumulation of triglycerides in high-fed diet rats' salivary glands, signifying the atrophy and malfunctions [1]. Moreover, an association between Sjögren's syndrome and obesity-related metabolic disorders was established. In this context, Shikama et al. demonstrated that saturated fatty acids provoked pro-inflammatory and apoptotic responses in human salivary gland epithelial cells [37]. Another clinical study observed morphological alteration in salivary glands of diabetic patients, such as increased acinar and granular size, reduced mitochondrial size, increased density of protrusions and microbuds, and luminal membranes [38].

4.2. Morphometric analysis

Morphometric analysis helped to quantitatively measure the effects of regular vitamin D and nano vitamin D on the fatty salivary gland, thereby adding qualitative descriptive histological evidence. The digital image analysis supported the histological data where the high-fat diet caused a state of hypertrophy (approximately 1.4-fold increase in size) in the serous acini cells, along with a 3-fold reduction in the cell number, coupled with a marked reduction (approximately 13-fold) in the number of serous secretory granules with a reduced size (greater than 3-fold reduction in size). The number of mucous secretory granules was also found to increase significantly (greater than 2-fold increase compared to that in the untreated or healthy diet groups). A profound effect on the mucous granule size (greater than 5-fold reduction in size compared to that of the untreated group) was observed, indicating that the increase in the number of mucous granules may be due to a compensatory mechanism to overcome the degeneration of the mucous acini.

Notably, a high-fat diet causes the number and size of serous secretory granules to decrease. However, the number of mucous secretory granules increased, despite severe reductions in size. Thus, a high-fat diet evidently causes both the serous and mucous acini to degenerate. However, there are clear and marked histological and structural differences between the two. The serous acini are primarily responsible for producing a watery fluid and specialized proteins, such as alpha-amylase and immunoglobulins, whereas the mucous acini produce a thick fluid with mucins [39]. Mucins are part of a thick substance called mucous, containing fats that cover and protect all mucosal surfaces in the body, including the oral cavity [40]. Lipids are an essential component of saliva and are present in healthy individuals. However, the levels and types of fats may vary across diseases, including diabetes [1].

Vitamin D is a fat-soluble vitamin packaged into chylomicrons and transported throughout the blood to the liver followed by the target tissues after absorption into the gastrointestinal tract. Previous studies have indicated that vitamin D is internalized at higher levels in epithelial cells, striated ducts, myoepithelial cells, and other salivary gland structures compared to the mucous and serous acini [32]. Myoepithelial cells are contractile components that promote saliva secretion and expulsion. They have also been recognized as targets of vitamin D. The effect of regular vitamin D and nano vitamin D treatment is more apparent on the serous acini than the mucous acini, presumably because serous tissue requires, stores, and processes less fat than mucous tissue [41].

Treatment of the submandibular and sublingual glands with regular vitamin D enhances its function by improving the following functions of myoepithelial cells: (1) transporting metabolites to the acini cells [42]; (2) reinforcing the underlying parenchyma and preventing damage; (3) playing a crucial role in regulating electrolyte exchange between stroma and lumen; and (4) aiding in the propagation of secretion and other stimuli [43]. Vitamin D also plays a role in the renewal of intercalated duct cells as it contains stem cells [44]. Although very little is known about the role of vitamin D in fostering mucous secretions, it is known to play an active role in promoting calcium-induced serous salivary flow [45]. Furthermore, previous studies have reported the anti-inflammatory effects of vitamin D [46, 47].

Our study confirmed that treatment with regular vitamin D reduces inflammation, indicated by reduced immune cell infiltration. However, we also found that nano vitamin D was superior to conventional vitamin D as an anti-inflammatory agent. The nano-emulsion formulation of vitamin D has been previously reported to be far superior to regular vitamin D at protecting against the effects of nonalcoholic fatty liver disease [23]. As shown in this study, these findings are mirrored in the case of fatty degenerated salivary glands, particularly in serous tissue.

We expect the uptake of vitamin D by serous acini to be better than that bymucous acini; hence, its protective effect is evident on the submandibular gland compared to the sublingual gland. In the present study, the enhanced protective effect of nano vitamin D was found to be superior to that of regular vitamin D, showing better absorption, increased solubility and stability, greater half-life, non-toxicity, and better bioavailability. However, further studies will be needed to confirm the results presented herein.

5. Conclusion

A nano-emulsion of vitamin D was found to produce better results than regular vitamin D in terms of its protective effects against HFD-induced submandibular and sublingual gland inflammation and degeneration in a rat model.

Declarations

Author contribution statement

Rasha Hamed Al-Serwi, Mohamed El-Sherbiny, Mohamed Ahmed Eladl, Ashwag Aloyouny, Ishrat Rahman: Conceived and designed the experiments; Performed the experiments; Analyzed and interpreted the data; Contributed reagents, materials, analysis tools or data; Wrote the paper.

Funding statement

This work was supported by the Deanship of Scientific Research at Princess Nourah bint Abdulrahman University (Fast-track Research Funding Program).

Data availability statement

Data included in article/supplementary material/referenced in article.

Declaration of interests statement

The authors declare no conflict of interest.

Additional information

No additional information is available for this paper.

References

[1] J. Matczuk, A. Zalewska, B. Łukaszuk, M. Knaś, M. Maciejczyk, M. Garbowska, D.M. Ziembicka, D. Waszkiel, A. Chabowski, M. Żendzian-Piotrowska, Insulin resistance and obesity affect lipid profile in the salivary glands, J. Diabetes Res. (2016) 1–9.
[2] K. Kurek, A. Mikłosz, B. Łukaszuk, A. Chabowski, J. Górski, M. Żendzian-Piotrowska, Inhibition of ceramide de novo synthesis ameliorates diet induced skeletal muscles insulin resistance, J. Diabetes Res. (2015) 1–9.
[3] K. Kurek, D.M. Piotrowska, P. Wiesiołek-Kurek, B. Łukaszuk, A. Chabowski, J. Górski, M. Żendzian-Piotrowska, Inhibition of ceramide de novo synthesis reduces liver lipid accumulation in rats with nonalcoholic fatty liver disease, Liver Int. 34 (2014) 1074–1083.
[4] A. Bonen, N. Tandon, J. Glatz, J. Luiken, G. Heigenhauser, The fatty acid transporter FAT/CD36 is upregulated in subcutaneous and visceral adipose tissues in human obesity and type 2 diabetes, Int. J. Obes. 30 (2006) 877–883.
[5] A. Hand, R.E. Weiss, Effects of streptozotocin-induced diabetes on the rat parotid gland, Lab. Invest. J. Tech. Methods Pathol. 51 (1984) 429–440.
[6] M.E. Ertunc, G.S. Hotamisligil, Lipid signaling and lipotoxicity in metaflammation: indications for metabolic disease pathogenesis and treatment, J. Lipid Res. 57 (2016) 2099–2114.
[7] A. Punj, Secretions of human salivary gland, in: Salivary Glands-New Approaches in Diagnostics and Treatment, IntechOpen, 2018.
[8] C.L. Maruyama, M. Monroe, J. Hunt, L. Buchmann, O.J. Baker, Comparing human and mouse salivary glands: a practice guide for salivary researchers, Oral Dis. 25 (2019) 403–415.
[9] J. Sheikh, M. Sharma, A. Kunath, D. Fritz, C. Glueck, E. Hess, Reversible parotid enlargement and pseudo-Sjögren's syndrome secondary to hypertriglyceridemia, J. Rheumatol. 23 (1996) 1288–1291.
[10] A.L. Mescher, Junqueira's Basic Histology: Text and Atlas, McGraw-Hill Education, 2018.
[11] H.R. Sandstead, C.J. Koehn, S.M. Sessions, Enlargement of the parotid gland in malnutrition, Am. J. Clin. Nutr. 3 (1955) 198–214.
[12] W.G. Hemenway, G.W. Allen, Chronic enlargement of the parotid gland; hypertrophy and fatty infiltration, Laryngoscope 69 (1959) 1508–1523.
[13] M. Izumi, K. Eguchi, H. Nakamura, S. Nagataki, T. Nakamura, Premature fat deposition in the salivary glands associated with Sjögren syndrome: MR and CT evidence, Am. J. Neuroradiol. 18 (1997) 951–958.
[14] A. Holland, G. Baron-Hay, B. Brennan, Parotid lipomatosis, J. Pediatr. Surg. 31 (1996) 1422–1423.
[15] L.M. Tartaglino, V.M. Rao, D.A. Markiewicz, Imaging of radiation changes in the head and neck, in: Seminars in Roentgenology, Elsevier, 1994, pp. 81–91.
[16] D.D. Bikle, Vitamin D metabolism, mechanism of action, and clinical applications, Chem. Biol. 21 (2014) 319–329.
[17] A.S. Kadappan, C. Guo, C.E. Gumus, A. Bessey, R.J. Wood, D.J. McClements, Z. Liu, The efficacy of nanoemulsion-based delivery to improve vitamin D absorption: comparison of in vitro and in vivo studies, Mol. Nutr. Food Res. 62 (2018) 1700836.
[18] V.K. Maurya, M. Aggarwal, Factors influencing the absorption of vitamin D in GIT: an overview, J. Food Sci. Technol. 54 (2017) 3753–3765.
[19] E. Šimoliūnas, I. Rinkūnaitė, Ž. Bukelskienė, V. Bukelskienė, Bioavailability of different vitamin D Oral supplements in laboratory animal model, Medicina 55 (2019) 265.
[20] C. de Oliveira, J.P. Biddulph, V. Hirani, I.J.C. Schneider, Vitamin D and inflammatory markers: cross-sectional analyses using data from the English Longitudinal Study of Ageing (ELSA), J. Nutr. Sci. 6 (2017).
[21] A. Nitsa, M. Toutouza, N. Machairas, A. Mariolis, A. Philippou, M. Koutsilieris, Vitamin D in cardiovascular disease, In Vivo 32 (2018) 977–981.
[22] H. Wang, W. Chen, D. Li, X. Yin, X. Zhang, N. Olsen, S.G. Zheng, Vitamin D and chronic diseases, Aging Dis. 8 (2017) 346.
[23] M. El-Sherbiny, M. Eldosoky, M. El-Shafey, G. Othman, H.A. Elkattawy, T. Bedir, N.M. Elsherbiny, Vitamin D nanoemulsion enhances hepatoprotective effect of conventional vitamin D in rats fed with a high-fat diet, Chem. Biol. Interact. 288 (2018) 65–75.
[24] L.S. Greene-Finestone, D. Garriguet, S. Brooks, K. Langlois, S.J. Whiting, Overweight and obesity are associated with lower vitamin D status in Canadian children and adolescents, Paediatr. Child Health 22 (2017) 438–444.
[25] J.E. Park, P.T. Pichiah, Y.-S. Cha, Vitamin D and metabolic diseases: growing roles of vitamin D, J. Obes. Metabol. Syndr. 27 (2018) 223.
[26] E. Benetti, R. Mastrocola, F. Chiazza, D. Nigro, G. D'Antona, V. Bordano, R. Fantozzi, M. Aragno, M. Collino, M.A. Minetto, Effects of vitamin D on insulin resistance and myosteatosis in diet-induced obese mice, PloS One 13 (2018).
[27] N. Jiang, Essays in Political Economy, University of Illinois at Urbana-Champaign, 2015.
[28] J.D. Bancroft, M. Gamble, Theory and Practice of Histological Techniques, Elsevier health sciences, 2008.
[29] A. Woods, Electron Microscopy: the Preparative Techniques, Churchill Livingstone, 2002.
[30] K.F. Badrealam, M. Owais, Nano-sized drug delivery systems: development and implication in treatment of hepatocellular carcinoma, Dig. Dis. 33 (2015) 675–682.
[31] J.K. Patra, G. Das, L.F. Fraceto, E.V.R. Campos, M. del Pilar Rodriguez-Torres, L.S. Acosta-Torres, L.A. Diaz-Torres, R. Grillo, M.K. Swamy, S. Sharma, Nano based drug delivery systems: recent developments and future prospects, J. Nanobiotechnol. 16 (2018) 71.
[32] W.E. Stumpf, N. Hayakawa, Salivary glands epithelial and myoepithelial cells are major vitamin D targets, Eur. J. Drug Metabol. Pharmacokinet. 32 (2007) 123–129.

[33] T.J. Lasisi, S.-T.T. Shittu, A.R. Alada, C. Physiology, Pharmacology, Re-establishing normal diet following high fat-diet-induced obesity reverses the altered salivary composition in Wistar rats, J. Basic Clin. Physiol. Pharmacol. 30 (2018) 111–120.
[34] A. Zalewska, Oxidative Modification in the Salivary Glands of High Fat-Diet Induced Insulin Resistant Rats.
[35] O. Amano, K. Mizobe, Y. Bando, K. Sakiyama, Anatomy and histology of rodent and human major salivary glands—overview of the Japan salivary gland society-sponsored workshop—, Acta Histochem. Cytoc. 45 (2012) 241–250.
[36] M. Kamata, M. Shirakawa, K. Kikuchi, T. Matsuoka, S. Aiyama, Histological analysis of the sublingual gland in rats with streptozotocin-induced diabetes, Okajimas Folia Anat. Jpn. 84 (2007) 71–76.
[37] Y. Shikama, N. Ishimaru, Y. Kudo, Y. Bando, N. Aki, Y. Hayashi, M. Funaki, Effects of free fatty acids on human salivary gland epithelial cells, J. Dent. Res. 92 (2013) 540–546.
[38] M.A. Lilliu, P. Solinas, M. Cossu, R. Puxeddu, F. Loy, R. Isola, M. Quartu, T. Melis, M. Isola, Medicine, Diabetes causes morphological changes in human submandibular gland: a morphometric study, J. Oral Pathol. Med. 44 (2015) 291–295.
[39] P.A. Wilmarth, M.A. Riviere, D.L. Rustvold, J.D. Lauten, T.E. Madden, L.L. David, Two-dimensional liquid chromatography study of the human whole saliva proteome, J. Proteome Res. 3 (2004) 1017–1023.
[40] L.A. Tabak, Structure and function of human salivary mucins, Crit. Rev. Oral Biol. Med. 1 (1990) 229–234.
[41] S.A. Selim, The effect of high-fat diet-induced obesity on the parotid gland of adult male albino rats: histological and immunohistochemical study, Egypt. J. Histol. 36 (2013) 772–780.
[42] J. Garrett, N. Emmelin, Activities of salivary myoepithelial cells: a review, Med. Biol. 57 (1979) 1–28.
[43] G.L. Ellis, P.L. Auclair, D.R. Gnepp, Surgical Pathology of the Salivary Glands: Volume 25 in the Major Problems in Pathology Series, WB Saunders Company, 1991.
[44] N. Koike, W.E. Stumpf, Sweat gland epithelial and myoepithelial cells are vitamin D targets, Exp. Dermatol. 16 (2007) 94–97.
[45] B. Glijer, C. Peterfy, A. Tenenhouse, The effect of vitamin D deficiency on secretion of saliva by rat parotid gland in vivo, J. Physiol. 363 (1985) 323–334.
[46] V.P. Hiremath, C.B. Rao, V. Naik, K.V. Prasad, Anti-inflammatory effect of vitamin D on gingivitis: a dose-response randomised control trial, Oral Health Prev. Dent. 11 (2013) 61–69.
[47] A.Q.H. Alkhedaide, Z.S. Alshehri, M.M. Soliman, K.W. Althumali, H.S. Abu-Elzahab, A.A.A. Baiomy, Vitamin D3 Supplementation Improves Immune and Inflammatory Response in Vitamin D Deficient Adults in Taif, Saudi Arabia, 2016.